

## Selective oxidation of ammonia to nitrogen over silica supported molybdena catalysts

### A structure-selectivity relationship

Mark de Boer<sup>a</sup>, A. Jos van Dillen<sup>a</sup>, Diederick C. Koningsberger<sup>a</sup>, Frans J.J.G. Janssen<sup>b</sup>, Tys Koerts<sup>c</sup> and John W. Geus<sup>a</sup>

<sup>a</sup> Department of Inorganic Chemistry, University of Utrecht, P.O. Box 80083, Sorbonnelaan 16, 3508 TB Utrecht, the Netherlands

<sup>b</sup> N.V. KEMA, P.O. Box 9035, 6800 ET Arnhem, the Netherlands

<sup>c</sup> Department of Inorganic Chemistry, Eindhoven University of Technology, Den Dolech 2, P.O. Box 513, 5600 MB, the Netherlands

### Abstract

The selective catalytic oxidation of NH<sub>3</sub> to N<sub>2</sub> over unsupported and silica-supported MoO<sub>3</sub> catalysts has been investigated. The defect structure of the catalysts greatly affects the selectivity towards N<sub>2</sub>O. The performance of the silica supported catalysts is controlled by the thermal pretreatment and the structure, which is installed by the preparation procedure. Water dramatically decreases the selectivity to N<sub>2</sub> of MoO<sub>3</sub>-on-SiO<sub>2</sub> catalysts with low loadings. The selectivity to N<sub>2</sub> highly depends on the ability of the catalyst to decompose released N<sub>2</sub>O, which proceeds on oxygen vacancies.

### 1. INTRODUCTION

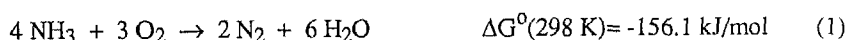
The emission of ammonia substantially contributes to the present air pollution. About 94 % of the ammonia emitted in, e.g., the Netherlands originates from agricultural sources [1]. In areas with intensive stock breeding emission of ammonia leads to acidification of the atmosphere. Large volumes of ammonia are additionally produced in coal gasification and hydrotreating plants. If the NH<sub>3</sub> produced is subsequently converted to nitrogen oxides, the environments will be comparably adversely affected.

Many studies have been dedicated to the Selective Catalytic Reduction (SCR) of NO<sub>x</sub> with NH<sub>3</sub>. Silica- and titania-supported V<sub>2</sub>O<sub>5</sub> catalysts have proven to perform adequately in the abatement of NO<sub>x</sub> [2,3]. A severe difficulty of the SCR is the stoichiometric amount of NH<sub>3</sub> with respect to NO<sub>x</sub> that must be injected and thoroughly mixed into the gas stream to avoid slip of either NH<sub>3</sub> or NO<sub>x</sub>.

The Selective Catalytic Oxidation (SCO) of NH<sub>3</sub> can meet with the removal of NH<sub>3</sub> from stack gases. Molecular oxygen is used for the selective oxidation of NH<sub>3</sub> to N<sub>2</sub> and H<sub>2</sub>O

(reaction 1). However, besides the desired products, i.e.,  $N_2$  and  $H_2O$ , also  $N_2O$  and  $NO$  can result (reactions 2-3). A number of catalysts can be used for the SCO [4]. Some -unsupported- transition metal oxides, such as,  $MoO_3$ ,  $V_2O_5$ ,  $Bi_2O_3$  and  $PbO$ , exhibit a sufficient selectivity towards  $N_2$ .

Thermodynamically, molecular nitrogen is the most stable reaction product [5]. A sequential oxidation path to the deepest oxidation product with  $N_2$  and  $N_2O$  as intermediate products (reaction 4) can therefore be excluded at the temperatures of interest (below 700 K).



The catalytic oxidation of  $NH_3$  is presumed to proceed by a reduction-oxidation mechanism [6], in which the reduction-oxidation behaviour of the catalyst affects the catalytic performance. According to Golodets [4], the bond energy of lattice oxygen within the bulk oxides determines mainly the selectivity ratio ( $N_2/N_2O+NO$ ), if a parallel reaction scheme is assumed (reaction 1-3).



Baiker *et al.* [7] found that the selectivity of the SCR reaction over annealed  $MoO_3$  samples highly depends on the grain morphology and the exposed lattice planes. Depending on the preparation procedure, samples with different distributions of exposed lattice planes can be produced. A sample with predominantly exposed (010) planes appeared to be less selective for the formation of  $N_2O$  in the SCR reaction than a sample exposing more (100), (001) and (101) faces. Gandhi *et al.* [8] investigated the influence of  $H_2O$  on the performance of copper(II) molybdate catalysts in the selective oxidation of  $NH_3$  to  $N_2$ . Addition of  $H_2O$  reduces the activity of these catalysts due to competitive adsorption of  $H_2O$  on sites active for  $NH_3$  adsorption. The selectivity for  $N_2$  decreases as well. Thus, Baiker proved that, in addition to its chemical characteristics, the catalytic properties of a compound strongly depend on its surface texture. This simply explains why the preparation conditions affect the catalytic performance. It may be expected that with supported catalysts this effect is even more pronounced, because the texture of the supported particles of the catalytically active component strongly depends on the preparation conditions. A number of additional features controls on the performance in the selective oxidation of  $NH_3$  to  $N_2$  as well. The structure of the catalyst particles, the reduction behaviour, and thermal pretreatment are important parameters.

Supported catalysts, such as,  $WO_3/TiO_2$  and  $Fe_2O_3/SiO_2$ , have appeared to be fairly selective in the oxidation of  $NH_3$  to  $N_2$ , but exhibit a poor activity. In this paper, the catalytic performance of a number of silica-supported  $MoO_3$  catalysts will be dealt with. The influence on the selectivity of the structure of the catalysts as determined with various characterisation techniques, will be discussed and compared with that of some unsupported  $MoO_3$  catalysts.

## 2. EXPERIMENTAL

### 2.1. Preparation of the Catalysts

The MoO<sub>3</sub>-on-SiO<sub>2</sub> catalysts were prepared by deposition of a molybdenum precursor from homogeneous solution onto SiO<sub>2</sub> (aerosil 200V, Degussa) as described by Geus [9]. To establish a sufficiently high positive interaction between the active phase and the support a precursor of a lower valence was used (Mo<sup>III</sup>Cl<sub>6</sub><sup>3-</sup>), prepared by electrochemical reduction of H<sub>2</sub>MoO<sub>4</sub> in concentrated HCl. It has been well documented that the preparation of MoO<sub>3</sub>/SiO<sub>2</sub> catalysts from a hexavalent ammonium heptamolybdate (AHM) precursor leads to the formation of fairly large MoO<sub>3</sub> crystallites [10-14] due to its poor interaction with silica. The merely anionic, dissolved (hexavalent) molybdenum species (Mo<sub>7</sub>O<sub>24</sub><sup>6-</sup> and Mo<sub>8</sub>O<sub>26</sub><sup>4-</sup> [15]) have no interaction with the SiO<sup>-</sup> groups on the surface of the support. Therefore, thus prepared catalysts usually exhibit the catalytic features of bulk MoO<sub>3</sub>. The interaction of trivalent molybdenum with SiO<sub>2</sub> is much better, because of the lower acidity of this precursor.

Precipitation of the active phase was brought about by slow injection of a 5% NH<sub>3</sub>-solution into a vessel containing Mo<sup>III</sup>Cl<sub>6</sub><sup>3-</sup> in an aqueous SiO<sub>2</sub> suspension. Homogeneity was ensured by vigorous stirring and the presence of baffles in the vessel. When the pH had reached the level of 7.0, the injection was stopped, the slurry was filtered off, and washed with demineralised water. The catalysts were dried in air at 393 K for 16 hours, and calcined in air at 723 K for 72 hours.

Unsupported MoO<sub>3</sub> catalysts were obtained by precipitation of Mo<sup>III</sup>Cl<sub>6</sub><sup>3-</sup> from a homogeneous solution without suspended SiO<sub>2</sub> (*type 1*: precipitated) or purchased from Cerac (ultrapure quality) (*type 2*: annealed). Both unsupported catalysts were calcined at 723 K.

### 2.2. Characterisation of the catalysts

The catalysts were characterised by various techniques: Thermal Analysis (TA), X-ray Photoelectron Spectroscopy (XPS), Raman Spectroscopy, and Extended X-ray Absorption Fine Structure (EXAFS). A short description of the experimental procedures is given.

Thermal Analysis experiments were performed within a Mettler TA-2 balance in a 10% H<sub>2</sub>/Ar flow (100 ml/min.). A sample of typically 50 mg of the powder was subjected to a temperature program (rate: 5 K/min.). The weight loss between 673 and 1073 K was used to calculate the degree of reduction of the samples.

Raman experiments were executed in a triplemate Spex (1877 model) spectrometer, coupled to an optical multichannel analyzer (Princeton Applied Research, model 1463) equipped with a intensified photodiode array detector. The 514.5 nm line of an Argon laser (Spectra Physics) was used as an excitation source. The sample was pressed into KBr and spun at 2000 rpm. The experiments were done under ambient conditions at a laser power of 10-50 mW.

The XPS-experiments were accomplished in a VG-Scientific Escalab MK II with a Mg K<sub>a</sub> source (1253.6 eV). The position of the peak maxima could be determined with an accuracy of ± 0.1 eV. The spectra were corrected for static charging effects with the C (1s) peak as an internal reference.

The X-ray absorption spectra in the EXAFS region (Mo K-edge at 19,999 eV) were measured at station 9.2 of the S.R.S. laboratory in Daresbury (U.K.). The storage ring was handled at 2.0 GeV with a ring current of 150-200 mA. A Si(220) crystal was used as the monochromator. Samples were crushed and pressed into a sample holder. Spectra were recorded at 290 K in helium atmosphere.

### 2.3. Kinetic Measurements

After calcination the catalysts were pelleted at 400 MPa for two minutes and subsequently crushed and sieved into the fraction range of 0.25-0.50 mm. The amount of catalyst was typically 100 mg. The catalysts were treated *in situ* at 673 K in a flow of 25 % O<sub>2</sub> in helium for two hours prior to the kinetic measurements. Mixtures of NH<sub>3</sub>/He, NO/He, O<sub>2</sub>/He, and high-purity helium were purchased from Air Products and used without further purification. The experiments were carried out at atmospheric pressure in a fixed bed reactor made of quartz. A Leybolt Q 200 mass spectrometer was used for detection of the reactants and products. The detection limit for the various products was 1 ppm. In some experiments NO was added to the feed to investigate the interference of this compound with the SCO reaction.

The performance of the MoO<sub>3</sub>/SiO<sub>2</sub> catalysts was also tested under non-stationary conditions. The catalysts, after prolonged exposure to ambient atmosphere (i.e., hydrated conditions), were submitted to a temperature program of 10 K/min in a flow of 5000 ppm NH<sub>3</sub>, 2 % O<sub>2</sub> and 97.5 % He. The LHSV was 12,000 hr<sup>-1</sup>.

## 3. RESULTS

### 3.1. Preparation and characterisation of the catalysts

A number of unsupported and silica-supported MoO<sub>3</sub> catalysts was prepared according to the procedures described in the experimental section. Table 1 presents the codes and the metal oxide loadings (defined as  $\frac{wt\ MoO_3}{wt\ MoO_3 + SiO_2} \cdot 100\%$ ) of the samples, as determined by Inductively Coupled Plasma analysis (ICP).

Table 1  
Properties of the catalysts

code	catalyst	preparation	loading (%)
Mo (prec.)	MoO <sub>3</sub>	HDP <sup>1</sup>	-
Mo (ann.)	MoO <sub>3</sub>	MoO <sub>3</sub> annealed	-
Mo6	MoO <sub>3</sub> /SiO <sub>2</sub>	HDP <sup>1</sup>	5.6
Mo11	MoO <sub>3</sub> /SiO <sub>2</sub>	HDP <sup>1</sup>	11.3
Mo26	MoO <sub>3</sub> /SiO <sub>2</sub>	HDP <sup>1</sup>	26.0

<sup>1</sup> Homogeneous Deposition Precipitation

The reduction profiles as obtained from TA-experiments are shown in figure 1. A significant difference in onset temperature of reduction of the two bulk-MoO<sub>3</sub> samples (*d* and *e*) is observed. Although these samples are chemically identical, their reduction behaviour is quite different. X.R.D.-analysis gave no elucidation of a possible difference in exposed lattice planes in the bulk samples. The explanation of the different reduction characteristic can be found in the

heterogeneity of the surface of the  $\text{MoO}_3$  samples. Van den Berg *et al.* [16] have shown that the activity for  $\text{CO}$ - and  $\text{H}_2$ -oxidation on  $\text{V}_2\text{O}_5$  catalysts and vanadium bronzes strongly depends on the concentration of defects in the  $\text{V}_2\text{O}_5$ -lattice (usually oxygen-vacancies). The catalytic reaction at high temperature proceeds via a reduction-oxidation mechanism, in which oxygen vacancies are the active species. Thus, it is feasible that a high concentration of defects in an oxidic lattice like  $\text{V}_2\text{O}_5$  or  $\text{MoO}_3$  locally destabilises the lattice and thus enhances the activity for an oxidation reaction. Since the TA-experiment in  $\text{H}_2$ -atmosphere can be envisioned to be an oxidation of  $\text{H}_2$  by the catalyst, the concentration of surface defects will control the onset temperature of the reduction of the catalyst. The lower onset temperature of  $\text{Mo}(\text{prec.})$  can thus be explained by its higher content of defects due to the preparation procedure: precipitation of molybdenum (hydr)oxide from an aqueous solution yields a porous, badly crystallised solid even after calcination. The heterogeneity of  $\text{Mo}(\text{prec.})$  is considerably higher than that of  $\text{Mo}(\text{ann.})$ , which contains annealed, well crystallised, stoichiometric  $\text{MoO}_3$  particles.

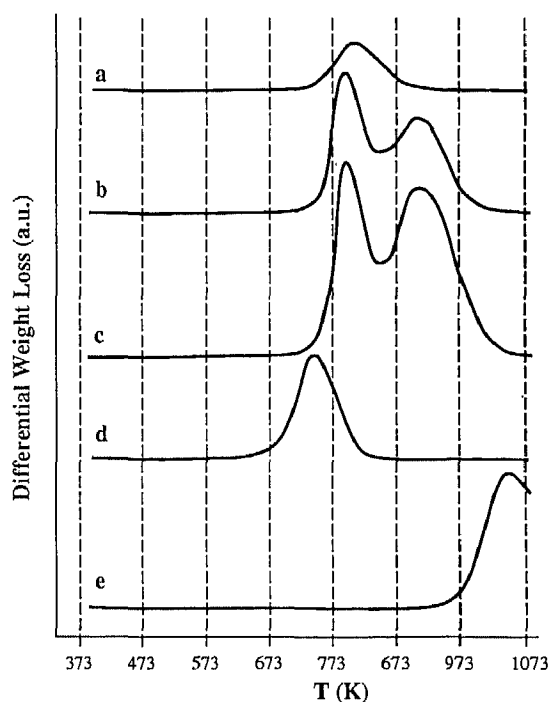


Figure 1 Thermogravimetric analysis of a)  $\text{Mo}_6$ , b)  $\text{Mo}_{11}$ , c)  $\text{Mo}_{26}$ , d)  $\text{Mo}(\text{prec.})$ , and e)  $\text{Mo}(\text{ann.})$  in a 10 %  $\text{H}_2/\text{Ar}$  flow.

The onset temperatures of Mo6, Mo11, and Mo26 (*a-c*) are equal, but the shape of the peaks and the integrated weight loss deviate strongly. Mo11 and Mo26 both exhibit a second peak at high temperature, which corresponds to deep reduction to metallic molybdenum, as evidenced by High Temperature XRD experiments. Mo6, however, has no peak at high temperatures and can be reduced less profoundly. with XPS, it was checked, that in all samples molybdenum is initially present in 6+ oxidation state. The Mo ( $3d_{5/2}$ ) peak is located at 232.8 eV. The reference values of the binding energy of the photoelectrons in MoO<sub>3</sub> and MoO<sub>2</sub> are 232.5 and 229.2 eV respectively. From the TG and XPS results we have calculated that Mo6 can be reduced only for 35%, whereas Mo11 and Mo26 can almost completely be reduced.

The Raman spectra of Mo6, Mo11, Mo26, and Mo (ann.) are represented in figure 2. The main bands of Mo (ann.) are positioned at  $\tilde{\nu}$ = 996, 821, 668, 285 and 159 cm<sup>-1</sup>; This corresponds with the literature values of bulk MoO<sub>3</sub> [17]. Obviously Mo11 and Mo26 contain crystalline MoO<sub>3</sub>. Mo6, however, has a distinctly different structure: the bands at  $\tilde{\nu}$ = 944, 880 and 220 cm<sup>-1</sup> indicate the presence of oligomeric molybdenum oxide clusters (comparable to aqueous hepta/ octamolybdate) [18]. The Raman bands at 480 and 370 cm<sup>-1</sup> are due to SiO<sub>2</sub> and a surface molybdenum oxide respectively.

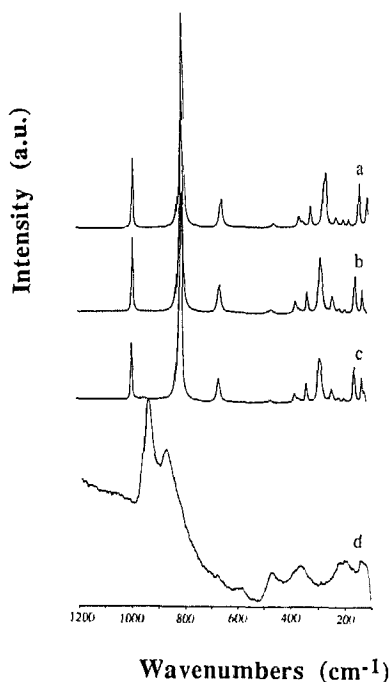


Figure 2 Raman spectra of a) Mo (ann.), b) Mo26, c) Mo11, and d) Mo6, recorded at ambient conditions

The results of a preliminary EXAFS study reveal analogous results. The amplitude of a  $k^1$  fourier transform of the  $\chi(k)$  is shown in figure 3. The Mo-Mo shell in Mo(ann.) is positioned at approx. 3.5 Å and originates from a strong Mo-Mo contribution, diagnostic for the existence of larger molybdenum oxide particles with long range order. The Mo-O peak at 1.5 - 2.2 Å is ascribed to more than one Mo-O distance due to distortion of the octahedral environment of the absorber. The same pattern is observed for Mo11 and Mo26: The Fourier transform of Mo6, however, deviates dramatically from the bulk reference. It reveals hardly any long range order, as evidenced by the decrease of the Mo-Mo contribution at ~3.5 Å.

The combined results of the characterisation of the catalysts show that Mo11 and Mo26 contain crystalline molybdenum(VI) oxide particles, highly dispersed onto the SiO<sub>2</sub> support, whereas Mo6 consists of very small molybdenum oxide clusters strongly interacting with the support. The different reduction behaviour of Mo6 is presumably caused by the strong interaction with the support: the tiny molybdenum oxide particle cannot be reduced to metallic molybdenum. Consequently, the reduction behaviour, i.e., the onset temperature and the maximum degree of reduction depend on the structure of the catalyst.

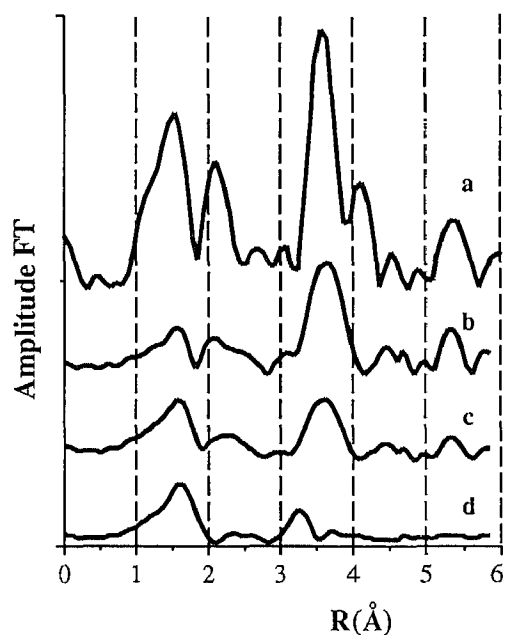


Figure 3 EXAFS  $k^1$  fourier transforms of  $\chi(k)$  ( $3.45 \text{ \AA}^{-1} < k < 12.9 \text{ \AA}^{-1}$ ) of a) Mo (ann.), b) Mo26, c) Mo11, and d) Mo6

### 3.2. Kinetic experiments

Ammonia oxidation experiments were performed over Mo (ann.) and Mo (prec.) in the presence of NO. The concentration profiles as a function of the temperature are shown in figure 4.

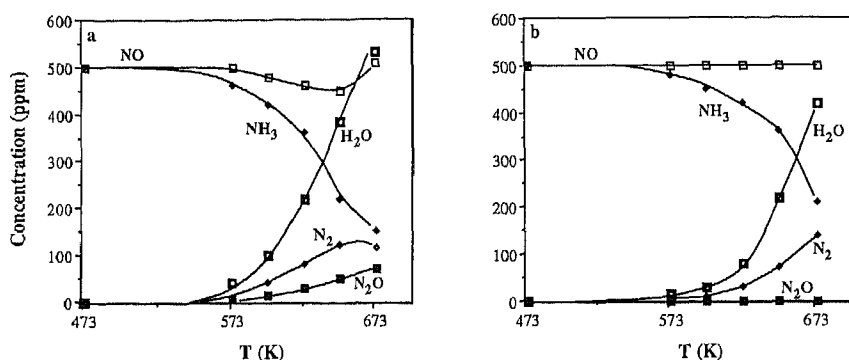


Figure 4 Concentration profiles of NH<sub>3</sub>, NO, N<sub>2</sub>, N<sub>2</sub>O and H<sub>2</sub>O in the NH<sub>3</sub>-oxidation over a) Mo (ann.), and b) Mo (prec.)

Despite the chemical equivalence of the two samples, their catalytic performance is quite different. The NH<sub>3</sub>-conversion at 673 K of Mo (ann.) is somewhat higher than Mo (prec.). The selectivity towards N<sub>2</sub>, however, is almost 100% up to 673 K for Mo (prec.), whereas Mo (ann.) produces a considerable amount of N<sub>2</sub>O. Moreover, NO is reactive with Mo (ann.) and remains unaffected with Mo (prec.). It is interesting to note that the minimum for NO in Mo(ann.) is associated with a maximum in N<sub>2</sub>. Apparently the formation of NO and N<sub>2</sub> from NH<sub>3</sub> is non-independent.

The results of the catalytic performance tests of the MoO<sub>3</sub>/SiO<sub>2</sub> catalysts are presented in figure 5. The selectivity of Mo6 strongly deviates from Mo11 and Mo26. Mo6 produces a substantial amount of nitrous oxide (33% of the amount of NH<sub>3</sub> converted), whereas Mo11 and Mo26 produce only 8 and 5% N<sub>2</sub>O respectively. With Mo6 formation of NO proceeds at temperatures above 773 K, which is accompanied by a decrease of the selectivity for N<sub>2</sub>O. This observation suggests that the formation of N<sub>2</sub>, N<sub>2</sub>O, and N<sub>2</sub> is interdependent, and that the reaction mechanisms for the formation of these products do not run completely parallel.



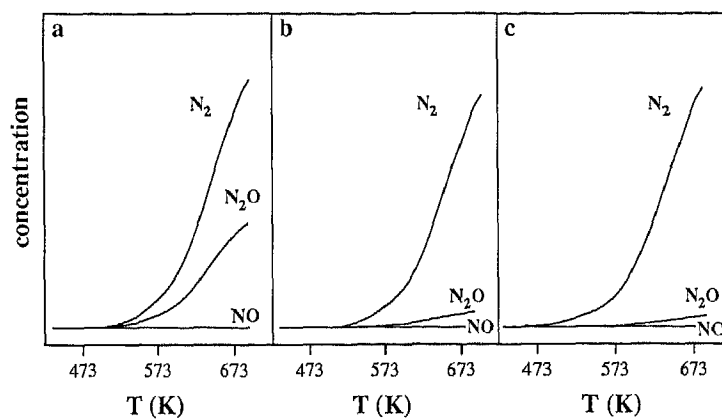


Fig. 5 formation of  $N_2$ ,  $N_2O$  and  $NO$  over a) Mo6, b) Mo11, and c) Mo26

These measurements were performed on fresh, calcined samples and, thus, contain adsorbed  $H_2O$  due to prolonged exposure to the ambient atmosphere. The selectivity of the catalysts drastically increases after a thermal pretreatment in  $O_2$  at 673 K. Table 2 shows the selectivities of the catalysts for the production of  $N_2$  at 673 K before and after thermal treatment.

Table 2  
Selectivities to  $N_2$  at 673 K

catalyst	selectivity	
	fresh	after pretreatment
Mo6	67	>98
Mo11	92	>98
Mo26	95	>98

The origin of the low selectivity of the fresh samples will next be discussed.

#### 4. DISCUSSION

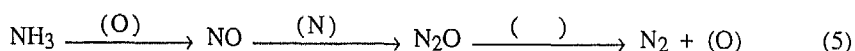
The reduction behaviour of Mo (ann.) and Mo (prec.) exhibits large differences. It has been mentioned that the onset temperature for the reduction of the samples strongly depends on the

concentration of lattice defects present at the surface of catalyst particles and the ability of the oxide to accommodate vacancies. The different catalytic performance of the samples in the oxidation of  $\text{NH}_3$  can be explained along the same lines. The formation of each  $\text{N}_2$ -molecule requires two nitrogen atoms from different  $\text{NH}_3$ -molecules, which implies that a  $\text{NH}_3$ -molecule has to adsorb dissociatively in close proximity of another  $\text{NH}_3$ . The mobility of adsorbed N-species is low, as reported for  $\text{V}_2\text{O}_5/\text{TiO}_2$  catalysts [19]. The recombination probability of two adsorbed nitrogen atoms to form an  $\text{N}\equiv\text{N}$  bond is thus determined by the surface density of active sites. Active sites for this reaction are oxygen atoms capable of accepting the hydrogen atoms from  $\text{NH}_3$ , i.e., reducible under the conditions of the reaction. Mo (prec.) contains a high number of active sites for the SCO reaction, as evidenced by the low onset temperature of reduction in the TA-profile (figure 1). The selectivity to  $\text{N}_2$  is optimal, because of the high probability of recombination of two nitrogen atoms to form  $\text{N}_2$ .

The formation of nitrous oxide in Mo (ann.) is not caused by the sequential oxidation of evolved  $\text{N}_2$  to  $\text{N}_2\text{O}$  as discussed before (reaction 4). Golodets *et al.* [4] explain the formation of  $\text{N}_2\text{O}$  by assuming the reaction between two HNO species to form  $\text{N}_2\text{O}$  and  $\text{H}_2\text{O}$ . A number of species is schematically postulated in the model in figure 6.

Each unit on the surface ('cube') represents a surface oxygen atom, without taking specific lattice planes into account. An oxygen vacancy is symbolised by a pit. The adsorption of a  $\text{NH}_3$ -molecule in (1), or remote (2) from an oxygen vacancy is depicted in this model. We assume that an  $\text{NH}_3$ -molecule is adsorbed dissociatively on the  $\text{MoO}_3$  surface ('stripped') and tends to occupy an oxygen vacancy, if present. Adjacent surface oxygen atoms are transformed into OH-groups. Two vicinal OH groups (3) can form an oxygen vacancy under evolution of  $\text{H}_2\text{O}$  (4). The lattice oxygen can be replenished by gas phase  $\text{O}_2$ . Species 5 visualises the situation of Mo (prec.): two  $\text{NH}_3$ -molecules are adsorbed and stripped in proximity (hydrogen atoms not shown) and are evolved as  $\text{N}_2$  (6). When the concentration of active sites is low, then the nitrogen atoms remain isolated, either on the surface of  $\text{MoO}_3$  (2) or in a vacancy (1). In this case the recombination probability of nitrogen atoms is low and development of NO becomes likely (7). Two pathways for evolved NO are conceivable. It can react with another nitrogen species to form  $\text{N}_2\text{O}$  (7-8) or it is swept out of the reactor (at high temperatures). The high selectivity for  $\text{N}_2\text{O}$  of Mo (ann.) can thus be explained, because Mo (ann.) contains few, remote vacancies.

Implicitly, we have postulated a reaction path opposite to reaction 4, as presented in reaction 5.



The last step of reaction 5 is the subsequent decomposition of  $\text{N}_2\text{O}$  occurring preferentially on oxygen vacancies. The oxygen atom from  $\text{N}_2\text{O}$  can be conveniently accommodated in the  $\text{MoO}_3$ -lattice, while the energy-favourable  $\text{N}\equiv\text{N}$  bond can be formed. Shelef *et al.* [20] report on the formation and decomposition of  $\text{N}_2\text{O}$  on chromia catalysts. At high space velocities the evolved  $\text{N}_2\text{O}$  cannot decompose and is swept out of the reactor. Keenan *et al.* [21] and Vorotyntsev *et al.* [22] confirm that the decomposition of  $\text{N}_2\text{O}$  takes place on surface vacancies.

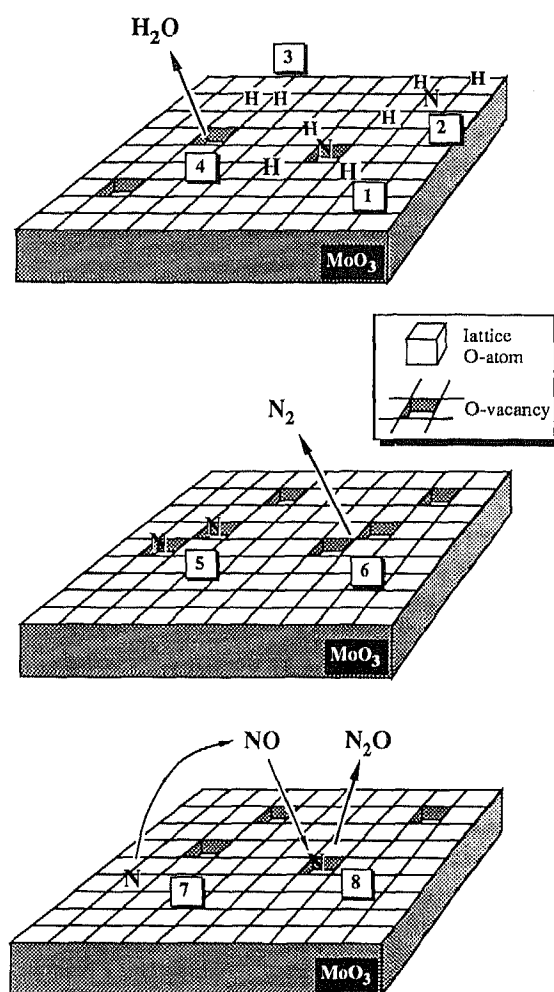


Figure 6 Schematic representation of surface species

The performance of the  $\text{MoO}_3/\text{SiO}_2$  catalysts is strongly affected by the presence of adsorbed  $\text{H}_2\text{O}$ . The molybdenum oxide phase and the silica are both hydroxylated. Since  $\text{H}_2\text{O}$  competes with  $\text{NH}_3$  for the adsorption on active sites [8], a smaller number  $\text{NH}_3$  molecules can be adsorbed and stripped in the presence of  $\text{H}_2\text{O}$ . Water leading to adsorbed hydroxyl

groups thus diminishes the concentration of adsorbed nitrogen species, which decreases the recombination probability of nitrogen atoms and enhances the selectivity towards  $N_2O$ .

This effect is far more pronounced with Mo6 than with Mo11 and Mo26, because of the different structure of the catalysts. The oligomeric molybdenum oxide clusters in Mo6 can only be reduced for approx. 35%. Only a limited number of  $NH_3$ -molecules can therefore be stripped, since the adsorption of each  $NH_3$  molecule requires the reduction of at least three oxygen atoms (formation of OH-groups). The recombination probability of nitrogen atoms and the rate of decomposition of  $N_2O$  are much higher on Mo11 and Mo26 under hydrated conditions as compared to Mo6. The larger  $MoO_3$  crystallites in Mo11 and Mo26 can more easily accommodate oxygen vacancies, because of their higher reducibility.

## 5. CONCLUSIONS

The activity and, more importantly, the selectivity of (un)supported  $MoO_3$  in the selective oxidation of  $NH_3$  to  $N_2$  appears to depend on the defect structure of the catalysts. The catalytic performance of the two unsupported  $MoO_3$  samples is controlled by the preparation procedure, which installs the reduction-oxidation properties and the selectivity to  $N_2$ . It is postulated that the selectivity for  $N_2$  is influenced by the recombination probability of adsorbed nitrogen atoms. The probability is high for catalyst particles with a high surface density of active sites. An active site for the selective oxidation of  $NH_3$  is an ensemble of reducible surface oxygen atoms in the vicinity of an oxygen vacancy. The oxygen atoms must strip the hydrogen atoms from  $NH_3$  to form OH groups. A vacancy is created when two vicinal OH groups desorb under release of  $H_2O$ . Surface oxygen is replenished by gas phase  $O_2$ . An adsorbed and stripped  $NH_3$ -molecule can react with another stripped nitrogen atom or immediately with a gas phase  $NH_3$ -molecule. Formation of the energetically favourable  $N\equiv N$  bond is the driving force for the recombination of two adsorbed nitrogen species. When no other nitrogen atom is in close proximity, NO can desorb.

$N_2O$  results when a NO molecule reacts with another isolated nitrogen atom. The participation of NO is demonstrated by addition of NO to the feed. The Mo (ann.) sample exhibits SCR behaviour. With isotopic experiments Janssen [19] proved that in the SRC reaction over vanadia catalysts the nitrogen atoms in  $N_2O$  originate from NO and  $NH_3$ . Formation of the undesired  $N_2O$  does not present problems, provided it consecutively decomposes under formation of  $N_2$  and an adsorbed oxygen atom. We believe that the selectivity of these catalysts is partly due to the capability to decompose undesired  $N_2O$ , which proceeds preferably at oxygen vacancies.

Since  $NH_3$  competes with  $H_2O$  for the active sites [8], the catalytic performance of hydrated samples is worse than that of thermally pretreated samples. The selectivity is significantly enhanced by a thermal pretreatment. The increase is most prominent for Mo6. Due to the small dimensions and poor reducibility of the oligomeric molybdenum oxide clusters only a limited number of  $NH_3$ -molecules can be stripped at the surface, thus decreasing the recombination probability. Decomposition of evolved  $N_2O$  cannot proceed because the required vacancies are occupied by water. The larger  $MoO_3$  crystallites in Mo11 and Mo26 can adsorb and strip more  $NH_3$  molecules and accommodate more vacancies for the decomposition of released  $N_2O$ .

## 6. ACKNOWLEDGEMENT

We thank I.E. Wachs and M. Vuurman for the performance of the Raman experiments.

## 7. REFERENCES

1. E.H.T.M. Nijpels, G.J.M. Braks, VROM 9031918-89 6974/118 (1989) 1
2. H. Bosch, F.J.J.G. Janssen, *Catal. Today*, 2 (1988) 369
3. E.T.C. Vogt, A. Boot, A.J. van Dillen, J.W. Geus, F.J.J.G. Janssen, F.M.G. van den Kerkhof, *J. Catal.*, 114 (1988) 313
4. G.I. Golodets Heterogeneous catalytic reactions involving molecular oxygen in: *Studies in Surface Science and Catalysis* (J.R. Ross ed.), Amsterdam, Elsevier 1983 p.312
5. I. Barin, O. Knacke, O. Kubaschewski, *Thermochemical properties of inorganic substances*, Berlin, Springer Verlag 1977
6. P. Mars, D.W. van Krevelen, *Spec. suppl. to Chem. Engin. Sci.*, 3 (1954) 41
7. A. Baiker, P. Dollenmeier, A. Reller, *J. Catal.*, 103 (1987) 394
8. H.S. Gandhi, M. Shelef, *J. Catal.*, 40 (1975) 312
9. J.W. Geus, *Production and thermal pretreatment of catalysts in: Studies in surface science and catalysis 16* (G. Poncelet, P. Grange, P.A. Jacobs (eds.)) Amsterdam, Elsevier 1983 p.1
10. T. Ono, M. Anpo, Y. Kubokawa, *J. Phys. Chem.*, 90 (1986) 4780
11. M. Anpo, M. Kondo, Y. Kubokawa, C. Louis, M. Che, *J. Chem. Soc., Faraday Trans. I.*, 84 (8) (1988) 2771
12. N. Kakuta, K. Tohji, Y. Udagawa, *J. Phys. Chem.*, 92 (1988) 2583
13. A. Latef, R. Elamrani, L. Gengembre, C.F. Aissi, S. Kasztelan, Y. Barbaux, M. Guelton, *Zeitschr. für Physikal. Chem. Neue Folge*, 152 (1987) 93
14. T-C. Liu, M. Forissier, G. Coudurier, J.C. Védrine, *J. Chem. Soc., Faraday Trans. I.*, 85 (7) (1989) 1607
15. C.F. Baes, R.E. Mesmer, *The hydrolysis of cations*, New York, J. Wiley & Sons 1976
16. J. van den Berg, A.J. van Dillen, J. van der Meyden, J.W. Geus in *Surface Properties and Catalysis by Non-Metals* (J.P. Bonnelle et al. (eds)) (1983)
17. H.M. Ismail, C.R. Theocharis, D.N. Waters, M.I. Zaki, R.B. Fahim, *J. Chem. Soc., Faraday Trans. 1.*, 83 (1987) 1601
18. J. Aveston, E.W. Anacker, J.S. Johnson, *Inorg. Chem.*, 3 (1964) 735
19. F.J.J.G. Janssen, F.M.G. van den Kerkhof, H. Bosch, J.R.H. Ross, *J. Phys. Chem.*, 91 (1987) 5921
20. M. Shelef, K. Otto, H. Gandhi, *J. Catal.*, 12 (1968) 361
21. A.G. Keenan, R.D. Iyengar, *J. Catal.*, 5 (1966) 301
22. V.M. Vorotyntsev, V.A. Shvets, V.B. Kazanskii, *Kinetika i Kataliz*, 12 (5) (1971) 1249